Synthesis, Spectroscopic and Electrochemical Properties and X-ray Studies of Bis(2,2′-bipyridyl)(3-(2-hydroxy-phenyl)-5-(pyridin-2-yl)-1,2,4-triazole)-ruthenium(II)hexafluorphosphate

R. HAGE, J. G. HAASNOOT*, J. REEDIJK

Department of Chemistry, Gorlaeus Laboratories, Leiden University, P.O. Box 9502, 2300 RA Leiden (The Netherlands)

R. WANG, E. M. RYAN, J. G. VOS

School of Chemical Sciences, Dublin City University, Dublin 9 (Ireland)

A. L. SPEK and A. J. M. DUISENBERG

Department of Chemistry, University of Utrecht, Padualaan 8, 3584 CH Utrecht (The Netherlands)

(Received December 7, 1989; revised February 19, 1990)

Abstract

A new ruthenium(II) bis(2,2′-bipyridyl) compound with 3-(2-hydroxy-phenyl)-5-(pyridin-2-yl)-1,2,4-triazole (H_2L) as co-ligand has been prepared and characterised by X-ray structure determination, NMR spectroscopy, electrochemical measurements, and UV–Vis absorption and emission spectroscopy. The compound of formula $[Ru(bpy)_2(HL)]PF_6 \cdot CH_3COCH_3$ crystallises in the monoclinic space group $P2_1/n$, with a = 14.242(1), b = 14.277(1), c = 17.968(1) Å, β = 97.27(1)° and Z = 4. The $Ru(bpy)_2$ moiety is bound to (HL) via N1 of the triazole ring (Ru–N = 2.051(3) Å) and N1 of the pyridine ring (Ru–N = 2.085(3) Å). The phenol group is connected to N4 of the triazole ring via intramolecular hydrogen bonding. pK_a titrations reveal that for free H_2L the pyridine ring, the triazole ring and the phenol group can be (de)protonated, but for the coordinated ligand, only a triazole- and a phenol-based protonation are observed. The cyclic voltammogram and differential pulse polarogram of the oxidation of the deprotonated compound show the presence of three oxidation steps; one ruthenium based and two phenol based. Protonation of the complex causes a large positive shift potential for oxidation of the ruthenium centre. All measurements agree with a phenolpyridyltriazole ligand having strong σ-donor properties.

Introduction

In recent years much attention has been paid to the synthesis and characterisation of new ruthenium compounds with diimine ligands [1–5]. Using a variety of techniques, the ground and excited states of $[Ru(bpy)_3]^{2+}$ (bpy = 2,2′-bipyridine) and related complexes have been examined extensively [6–11]. Through modification of the ligand structure, the spectroscopic and electrochemical properties of the complex have been altered. Most work has been devoted to six-membered bpy-like bidentate ligands. However, less work has focussed on pyridyl-azole ligands, such as pyridylpyrazole, pyridylimidazole and pyridyltriazole [12–18].

It is well established that the σ-donor properties of these ligands are stronger than those of bipyridine [12–18]. In ruthenium compounds containing such ligands this leads to a metal ion with a lower oxidation potential and as the π-acceptor properties of the pyridyltriazole ligands are weaker, such complexes also have more negative reduction potentials. These electronic properties of the ligands also induce a shift to higher energy of the MLCT (metal to ligand charge transfer) band. The emission quantum yield of the ruthenium complexes with pyridyl-azoles are in general lower than found for $[Ru(bpy)_3]^{2+}$ (bpy = 2,2′-bipyridine). This has been explained by a more efficient deactivation of the emitting ^{3}MLCT state via a metal centered state (^{3}MC) [4].

In the present work $Ru(bpy)_2$ complexes with a new ligand, 3-(2-hydroxy-phenyl)-5-(pyridin-2-yl)-1,2,4-triazole (H_2L) are reported (Fig. 1). The goal

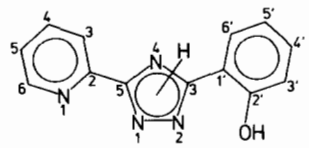

Fig. 1. 3-(2-hydroxyphenyl)-5-(pyridin-2-yl)-H-1,2,4-triazole (H_2L).

*Author to whom correspondence should be addressed.

0020-1693/90/$3.50

of this investigation is to obtain better insights into the relation between the structure and properties of ruthenium compounds through ligand modification. Furthermore the electronic effect of the presence of the phenol substituent on the electrochemical and photophysical properties of the complexes is investigated.

Experimental

Materials

Synthesis of 3-(2-hydroxy-phenyl)-5-(pyridin-2-yl)-H-1,2,4-triazole (H_2L)

Methylsalicylate was reacted with a slight excess of hydrazine, as described by Case [19]. The resulting salicoylhydrazine was refluxed with the methylimidate of picolinic acid for 2 h. Ring closure took place by heating the solid in ethylene glycol for 20 min [20]. The ligand was purified by crystallisation from ethanol (yield 60%).

^{1}H NMR data ($(CD_3)_2SO$): H3, 8.20(d); H4, 8.03(t); H5, 7.36(t); H6, 8.75(d); OH, 11.10(s); NH, 15.0(s); H3′, 8.03(m); H4′, 7.04(m); H5′, 7.56(t); H6′, 7.02(m) ppm.

Preparation of $[Ru(bpy)_2(HL)]PF_6$·acetone

$[Ru(bpy)_2Cl_2]$ (1 mmol) [21] was heated with 1.2 mmol of ligand in 50 ml of ethanol/water for 6 h. After evaporation to dryness, the solid was dissolved in 5 ml of water and precipitated in an aqueous NH_4PF_6 solution. The compound was purified by recrystallisation from water/acetone (1/1).

Anal. Calc. for $[Ru(C_{33}H_{25}N_8O)]PF_6 \cdot CH_3COCH_3$: C, 50.70; H, 3.64; N, 13.15; P, 3.64. Found: C, 50.78; H, 3.69; N, 13.18; P, 3.64%.

^{1}H NMR data of the coordinated HL-ligand ($(CD_3)_2CO$): H3, 8.24(+0.04); H4, 8.04(+0.01); H5, 7.32(−0.04); H6, 7.78(−0.97); OH, 11.40(+0.30); H3′, 7.98(−0.05); H4′, 6.78–6.84(−0.26/−0.20); H5′, 7.15(−0.41); H6′, 6.78–6.84(−0.24/−0.18).

Physical Measurements

Proton NMR spectra were obtained on a JEOL JNM-FX 200 MHz spectrometer or a Bruker 300 MHz spectrometer, ^{13}C NMR spectra on a JEOL 50.1 MHz spectrometer. All peak positions are relative to TMS.

The pK_a measurements were carried out on a Shimadzu UV-240 spectrophotometer. The emission titrations were obtained on a Perkin-Elmer LS-5 luminescence spectrophotometer equipped with a red-sensitive Hamamatsu R928 photomultiplier tube. An emission slit width of 10 nm was used and the data were not corrected for photomultiplier response.

A Britton-Robinson buffer (a mixture of 0.04 M in acetic acid, phosphoric acid and boric acid) was used as solvent for the pK_a and pK_a^* titrations. The compound was predissolved in a minimum amount of acetone or acetonitrile before addition to the buffer. The pH was adjusted by concentrated HCl or NaOH and measured by using a Corning 240 pH Meter.

Cyclic voltammetry (CV) was conducted using an EDT ECP 133 potentio/galvanostat together with a JJ PL3 X-Y recorder.

Differential pulse voltammetry (DPV) was carried out on an EG&G model 264A polarographic analyzer together with an EG&G G 2000 X-Y recorder.

Square wave voltammetry (SWV) was carried out on an EG&G model 273 potentio/galvanostat interfaced to a BBC microcomputer and linked with an Epson HI-80 plotter/printer.

HPLC-grade CH_3CN was used as solvent throughout the electrochemical measurements and it was dried over molecular sieves 4 Å and then filtered before use. Tetraethylammonium perchlorate (TEAP) was made by adding 70% $HClO_4$ to an aqueous tetraethylammonium bromide solution. The precipitate was collected by filtration, recrystallised three times from water and then dried at 50 °C in a vacuum oven overnight before use.

A 3 mm diameter teflon shrouded glassy carbon electrode was used as working electrode and a platinum electrode as auxiliary electrode. Ag/AgCl (saturated KCl) was used as reference electrode ($E^0_{Ag/AgCl(sat.KCl)}$ = 0.198 V versus NHE).

The electrochemical cell was a conventional three-compartment cell. It was degassed for 20 min with nitrogen in advance if the measurement was conducted below 0.0 V.

Unless stated otherwise, the electrolyte used was 0.1 M TEAP/CH_3CN. The scan rate was 100 mV/s in cyclic voltammetry and 5 mV/s in differential pulse voltammetry. The pulse height in differential pulse measurements was 50 mV.

Elemental analyses were carried out at University College Dublin.

X-ray Crystallography

A dark-red bar shaped crystal of dimensions 0.37 × 0.50 × 0.62 mm was selected for the X-ray analysis and mounted on a CAD4-F diffractometer. Crystal data and data collection parameters are presented in Table 1. The unit-cell parameters were determined by least-squares methods applied to the settings angles of 25 SET 4 reflections in the range 14–20° for θ. Data were collected at room temperature and have been corrected for Lorentz and polarisation effects.

Structure Solution and Refinement

The structure was solved by Patterson and Fourier methods (SHELXS-86) [22]. First isotropic and later on anisotropic thermal parameters were used for the non-hydrogen atoms. The hydrogen atoms were

TABLE 1. Experimental data for the X-ray diffraction study on $[Ru(bpy)_2(HL)]PF_6 \cdot CH_3COCH_3$

Formula	$C_{33}H_{25}N_8ORu \cdot PF_6 \cdot C_3H_6O$
Crystal system	monoclinic
Space group	$P2_1/n$
a (Å)	14.242(1)
b (Å)	14.277(1)
c (Å)	17.968(1)
β (°)	97.27(1)
Z	4
V (Å^3)	3624.1(4)
D_{calc} (Mg m^{-3})	1.565
D_m (Mg m^{-3})	1.56(1)
M_r	853.72
λ(Mo Kα) (Zr filtered) (Å)	0.71073
Linear absorption (cm^{-1})	5.4
$F(000)$	1728
Temperature (K)	295
Scan type	$\omega/2\theta$
Scan speed	0.60 + 0.35 tg θ
2θ range (°)	2.2–58.8
Reflections measured	h −19:19; k 0:19; l 0:24
Unique total data	9530
Unique observed data [$I > 2.5\sigma(I)$]	6322
R	0.048
R_w	0.059
S	1.64
w	$1/\sigma^2(F)$

introduced in calculated positions and refined with fixed geometries with respect to their carrier atoms. The final R (R_w) was 0.048 (0.059) with $R = \Sigma[(|F_o| - |F_c|)/\Sigma F_o]$ and $R_w = [\Sigma w(|F_o| - |F_c|)^2/\Sigma w|F_o|^2]^{1/2}$. The final difference maps showed no residual density other than a peak of 1.1 e/Å^3 near C13 indicating some positional disorder of the OH group. Scattering factors were taken from refs. 23 and 24. Final atomic coordinates for the non-hydrogen atoms are given in Table 2.

All calculations were carried out on a microVAX with the programs SHELX-76 [25] and PLATON [26].

Results and Discussion

Description of the X-ray Structure

Table 3 lists relevant bond distances and bond angles for the title compound. The distances and bonds angles of the atoms of the bipyridine ligands have not been tabulated, because these are normal for pyridine ligands. The Ru–N distances of 2.051(3)–2.085(3) Å observed in this structure are similar to those found in other ruthenium complexes [27–30].

As seen in Fig. 2, the metal centre is coordinated via N1 of the triazole ring and N7 of the pyridine

TABLE 2. Fractional atomic coordinates and isotropic thermal parameters (with e.s.d.s in parentheses) for the non-hydrogen atoms in the compound $[Ru(bpy)_2(HL)]PF_6 \cdot CH_3COCH_3$

Atom	x	y	z	U_{eq} (Å^2)[a]
Ru	0.25592(2)	0.67903(2)	0.37533(2)	0.0417(1)
O(18)	0.0830(4)	0.7009(4)	0.0123(2)	0.121(2)
N(1)	0.2166(2)	0.6563(2)	0.2630(2)	0.048(1)
N(2)	0.2593(2)	0.6200(2)	0.2053(2)	0.055(1)
N(4)	0.1237(2)	0.6950(2)	0.1584(2)	0.055(1)
N(7)	0.1237(2)	0.7436(2)	0.3576(2)	0.047(1)
N(20)	0.2877(2)	0.7296(2)	0.4827(2)	0.048(1)
N(26)	0.3212(2)	0.8034(2)	0.3557(2)	0.049(1)
N(40)	0.2072(2)	0.5489(2)	0.4024(2)	0.045(1)
N(46)	0.3785(2)	0.6023(2)	0.3861(2)	0.047(1)
C(3)	0.2010(3)	0.6451(3)	0.1437(2)	0.056(1)
C(5)	0.1378(3)	0.7003(3)	0.2340(2)	0.050(1)
C(6)	0.0824(3)	0.7468(3)	0.2850(2)	0.050(1)
C(8)	0.0745(3)	0.7813(3)	0.4103(2)	0.059(2)
C(9)	−0.0131(3)	0.8201(3)	0.3930(3)	0.072(2)
C(10)	−0.0532(3)	0.8239(4)	0.3195(3)	0.079(2)
C(11)	−0.0049(3)	0.7875(3)	0.2646(3)	0.066(2)
C(12)	0.2197(3)	0.6182(3)	0.0680(2)	0.061(2)
C(13)	0.2941(4)	0.5597(4)	0.0581(3)	0.082(2)
C(14)	0.3087(4)	0.5364(5)	−0.0149(3)	0.101(3)
C(15)	0.2497(5)	0.5708(5)	−0.0763(3)	0.097(3)
C(16)	0.1764(5)	0.6258(5)	−0.0661(3)	0.090(2)
C(17)	0.1614(4)	0.6498(4)	0.0058(3)	0.073(2)
C(21)	0.3351(3)	0.8121(3)	0.4883(2)	0.054(1)
C(22)	0.3574(4)	0.8564(4)	0.5573(3)	0.079(2)
C(23)	0.3306(4)	0.8141(5)	0.6202(3)	0.089(2)
C(24)	0.2849(4)	0.7314(5)	0.6142(3)	0.075(2)
C(25)	0.2643(3)	0.6894(3)	0.5459(2)	0.059(1)
C(27)	0.3576(3)	0.8518(3)	0.4172(2)	0.053(1)
C(28)	0.4134(3)	0.9307(3)	0.4120(3)	0.071(2)
C(29)	0.4313(4)	0.9608(4)	0.3426(3)	0.079(2)
C(30)	0.3909(4)	0.9143(3)	0.2798(3)	0.074(2)
C(31)	0.3376(3)	0.8377(3)	0.2889(3)	0.066(2)
C(41)	0.2729(3)	0.4799(3)	0.4098(2)	0.051(1)
C(42)	0.2504(3)	0.3904(3)	0.4288(3)	0.072(2)
C(43)	0.1591(4)	0.3682(4)	0.4410(3)	0.078(2)
C(44)	0.0923(3)	0.4384(3)	0.4329(3)	0.068(2)
C(45)	0.1182(3)	0.5264(3)	0.4142(2)	0.056(1)
C(47)	0.3691(3)	0.5098(3)	0.3994(2)	0.054(1)
C(48)	0.4468(3)	0.4497(4)	0.4039(3)	0.078(2)
C(49)	0.5346(3)	0.4854(4)	0.3965(3)	0.083(2)
C(50)	0.5440(3)	0.5794(4)	0.3869(3)	0.073(2)
C(51)	0.4661(3)	0.6363(3)	0.3815(3)	0.062(2)
O(60)	0.5390(5)	0.6917(5)	0.0801(3)	0.184(4)
C(61)	0.5419(4)	0.6708(6)	0.1427(4)	0.101(3)
C(62)	0.5514(7)	0.7406(5)	0.2056(5)	0.158(4)
C(63)	0.5403(6)	0.5709(6)	0.1696(5)	0.145(4)
P	0.6761(1)	0.0328(1)	0.17727(8)	0.0786(5)
F(1)	0.7409(3)	0.0343(4)	0.1148(2)	0.154(2)
F(2)	0.6251(3)	−0.0535(3)	0.1382(3)	0.142(2)
F(3)	0.6019(3)	0.0949(3)	0.1281(3)	0.169(3)
F(4)	0.7255(3)	0.1217(3)	0.2115(3)	0.172(2)
F(5)	0.6082(4)	0.0336(5)	0.2355(3)	0.221(3)
F(6)	0.7514(4)	−0.0300(4)	0.2201(3)	0.201(3)

[a] U_{eq} = 1/3 trace of orthogonalised $U_{i,j}$.

TABLE 3. Selected bond distances (Å) and angles (°) of $[Ru(bpy)_2(HL)]PF_6 \cdot CH_3COCH_3$

Ru–N1	2.051(3)	Ru–N7	2.085(3)
Ru–N20	2.056(3)	Ru–N26	2.056(3)
Ru–N40	2.063(3)	Ru–N46	2.049(3)
N1–N2	1.368(4)	N2–C3	1.346(5)
C3–N4	1.365(5)	N4–C5	1.350(5)
N1–C5	1.333(5)	C5–C6	1.444(6)
C6–N7	1.363(5)	N7–C8	1.358(5)
C8–C9	1.364(6)	C9–C10	1.372(7)
C10–C11	1.374(7)	C3–C12	1.470(5)
C12–C13	1.378(7)	C13–C14	1.394(8)
C14–C15	1.389(8)	C15–C16	1.337(10)
C16–C17	1.379(8)	C17–O18	1.351(8)
N1–Ru–N7	77.9(1)	N1–Ru–N20	168.3(1)
N1–Ru–N26	92.3(1)	N1–Ru–N40	91.8(1)
N1–Ru–N46	97.6(1)	N7–Ru–N20	94.3(1)
N7–Ru–N26	90.7(1)	N7–Ru–N40	96.3(1)
N7–Ru–N46	173.3(1)	N20–Ru–N26	78.9(1)
N20–Ru–N40	97.8(1)	N20–Ru–N46	90.9(1)
N26–Ru–N40	172.5(1)	N26–Ru–N46	94.6(1)
N40–Ru–N46	78.7(1)		

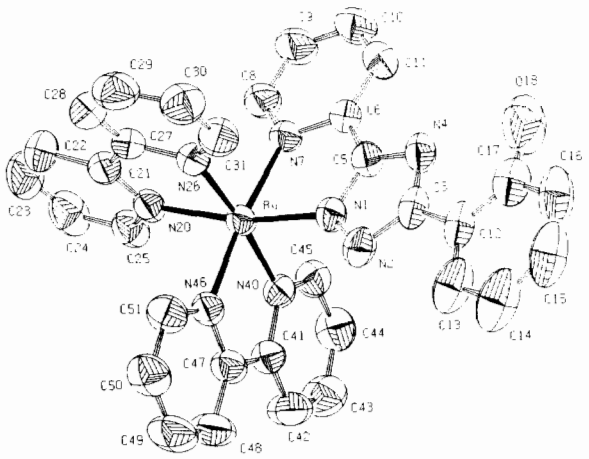

Fig. 2. Thermal motion ellipsoid plot (50% probability) of $[Ru(bpy)_2(HL)]^+$. Anion, solvent molecule and hydrogen atoms have been omitted for reasons of clarity.

ring. Previous work on ruthenium compounds containing various substituted pyridyltriazoles has revealed two coordination modes, viz. via N1 or via N4 of the triazole ring [17]. For the 3-substituted pyridyltriazole H_2L it is expected that only coordination via N1 occurs, because in this case less steric hindrance between the phenol group and the bulky bipyridine groups is present than when coordination via N4 would occur. A similar structure with 3,5-bis-(pyridin-2-yl)-1,2,4-triazole has been reported recently and in this structure coordination via N1 is also found [27].

The two bpy molecules are arranged in a *cis* geometry, as expected from the structure of *cis*-$[Ru(bpy)_2Cl_2]$ [28]. The phenol group is bound via a hydrogen bond to N4 with a N–O distance of 2.62(1) Å.

Proton NMR

The chemical shifts observed for the title compound have been listed in 'Experimental'. Using 2D-NMR techniques, the resonances of the asymmetric pyridyltriazole ligands could be assigned. The chemical shifts of the bipyridyl ligands are essentially the same as reported before [15, 17, 18, 31–36]. The resonances of the pyridyltriazole ligands are comparable to those of the previously reported methyl substituted pyridyltriazoles [16]. The H6 proton of the pyridine ring of the pyridyltriazole ligand has been shifted about 1 ppm upfield, which is caused by the anisotropic magnetic interaction of H6 with an adjacent pyridine ring [36]. The other protons are also shifted somewhat, because of the influence of the metal ion.

For the present work, NMR spectroscopy was not essential for elucidation of the structure of the compound, because the X-ray structure clearly revealed the coordination geometry around the metal centre and the various distances and angles. However, the present NMR data are of great use for similar structures where no X-ray data are available.

Acid–Base Properties

The acid–base chemistry of both the free ligand and of the ruthenium complex have been investigated. The pH dependence of the absorption spectrum of the title compound is given in Fig. 3(a) and (b). This Figure clearly shows the presence of two different protonation equilibria, one between pH 1 and 8, with isosbestic points at 385 and 455 nm, and the second one above pH 8, with isosbestic points at 385 and 473 nm. For the free phenolpyridyltriazole ligand three different protonation equilibria are observed. Two of these equilibria are shown in Fig. 4(a) and (b). These results can be explained by the presence of three protonation equilibria in the free ligand and two when the ligand is coordinated. The pK_a values calculated for these equilibria are given in Table 4, together with the absorption maxima of the different species. The pK_{a1} for the protonation of pyridine is 5.25 [37] and of bpy 4.45 [38], so it can safely be assumed that the lowest pK_{a1} value (3.22 ± 0.03) for the free H_2L ligand is due to the protonation of the pyridine ring. The next step (pK_{a2} = 6.00 ± 0.03) can be explained by deprotonation of the triazole ring [39], while finally above pH = 8, the deprotonation of the phenol substituent is expected to occur (pK_{a3} = 11.6 ± 0.5) [38].

By comparison with other similar systems, the first proton equilibrium observed for the complex (pK_{a1} = 3.72 ± 0.02) has been assigned to the protonation of the triazole ring [17, 18]. Table 4 shows clearly that

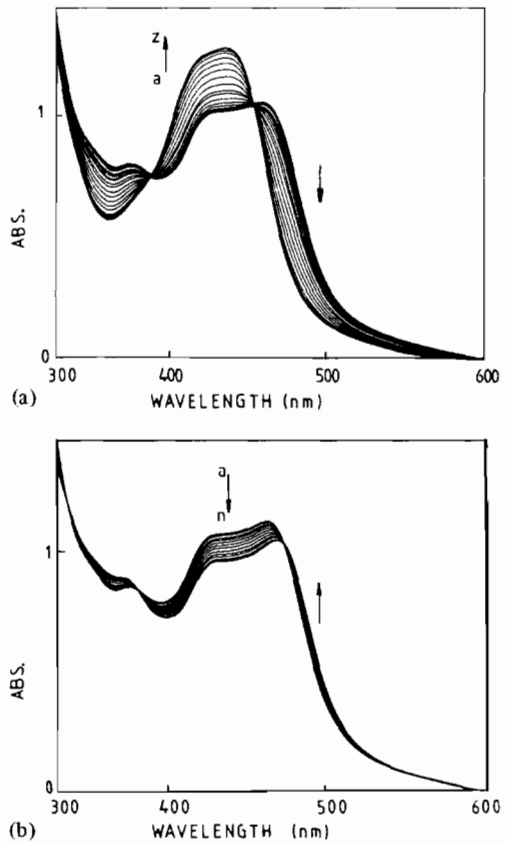

Fig. 3. pH dependence of the absorption spectrum of $[Ru(bpy)_2(HL)]PF_6$ (10^{-4} mol dm^{-3}) in an aqueous Britton-Robinson buffer: (a) for curves a to z pH = 7.35, 7.16, 6.95, 6.72, 6.56, 6.35, 6.07, 5.83, 5.56, 5.31, 5.06, 4.84, 4.61, 4.43, 4.21, 4.09, 3.89, 3.69, 3.49, 3.29, 3.10, 2.80, 2.58, 2.37, 2.15, 1.92; (b) for curves a to n pH = 9.54, 9.87, 10.23, 10.56, 10.85, 11.07, 11.27, 11.48, 11.70, 11.93, 12.14, 12.34, 12.54, 12.76.

the coordinated ligand is more acidic than the free ligand by about two orders of magnitude. On the other hand the deprotonation of the phenol group is not much affected by coordination to the $Ru(bpy)_2$ moiety. The increased acidity of the triazole ring upon coordination can be attributed to the σ-donor properties of the ring and to electrostatic effects of the charged complex versus the neutral ligand. The rather small reduction in pK_a of the phenol ring (about 0.5 pH units) points to a very limited interaction between the phenol group and the coordinating part of the ligand.

The effect of pH on the emission properties of the complex was also investigated. The pH dependence of its emission is given in Fig. 5. From the emission titration, inflection points, pH_i, of 3.27 ± 0.05 and 11.1 ± 0.1 respectively, were obtained. Unfortunately, it was impossible to measure the emission lifetimes of the different species. However, by using the room temperature emission wave lengths observed for the different species an estimate for the excited state pK_a, pK_a^* was made using the Förster cycle as in eqn. (1).

$$pK_a^* = pK_a + \frac{0.625(\nu_b - \nu_a)}{T} \quad (1)$$

where T is the absolute temperature, ν_b and ν_a are the energies in cm^{-1} of the (0–0) transition from the ground state to the excited state involved in the deprotonation equilibrium, for the base and acid forms, respectively [40].

With this formula a value of 2.7 was obtained for pK_{a1}^* and a value of 10.8 for pK_{a2}^*. By comparison with the values obtained for the corresponding ground state pK_as it appears that the excited state is more acidic than the ground state. This confirms the assumption that the triazole ligand is not directly involved in the excited state chemistry of the compound, but its photophysical properties of the complex are bpy based. Upon excitation the electron populates a bpy-based π^* orbital. This will create effectively a Ru(III) centre and consequently an increased electron donation from the pyridyltriazole ligand to the metal ion is present. Therefore, the lower excited state pK_a value compared with the ground state pK_a value indicates a bpy-based emission for this complex.

Electrochemistry

The differential pulse voltammogram of the oxidation of the free ligand H_2L shows two broad peaks at around 1.21 and 1.55 V versus Ag/AgCl (sat. KCl) in acetonitrile with 0.1 M TBAP. The electrochemistry of the phenol group has been studied in some detail and it is well known that the initially formed oxidation product undergoes a subsequent oxidation yielding the phenoxonium ion. The formation of dimers has also been reported resulting in an overall multi-electron oxidation process [41–44]. Furthermore, adsorption of the phenol group on the electrode surface and its oxidised products might also affect the charge transfer between the electrode and solution species. Because of the complexity of this electrochemistry the nature of the actual oxidation products was not further investigated. However, it seems likely that the first peak is caused by oxidation of the phenol group and the second peak by further oxidation of the products of the first oxidation process. Using cyclic voltammetry no reversible peak was observed for the reduction of the ligand up to −2.3 V. It is known that triazoles have weaker π^*-acceptor properties, and it is therefore very difficult to reduce the free ligands [17, 18, 39].

The differential pulse voltammogram of the ruthenium complex shows three oxidation peaks at 0.89, 1.26 and 1.44 V (Fig. 6) and two bpy-based reduction waves at −1.42 and −1.68 V (Table 5). By

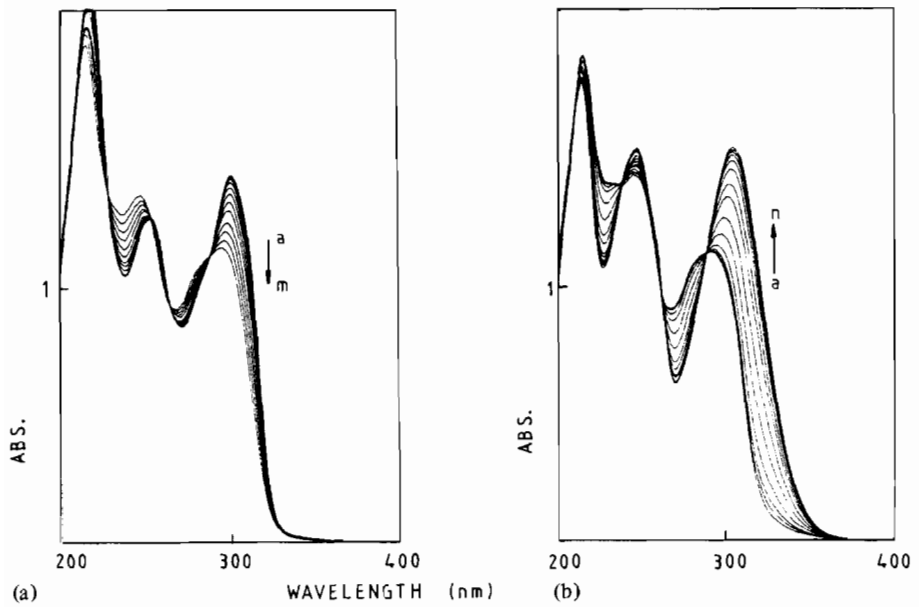

Fig. 4. pH dependence of absorption spectrum of H_2L in an aqueous Britton-Robinson buffer: (a) for curves a to m pH = 8.25, 8.00, 7.61, 7.36, 7.06, 6.82, 6.63, 6.43, 6.25, 6.03, 5.86, 5.67, 5.46; (b) for curves a to n pH = 4.48, 4.29, 4.12, 3.85, 3.55, 3.25, 2.97, 2.78, 2.51, 2.32, 2.13, 1.96, 1.80, 1.56.

TABLE 4. Acid–base properties of the free and coordinated 3-(2-hydroxy-phenyl)-5-(pyridine-2-yl)-1,2,4-triazole, obtained in a Britton-Robinson buffer

	Absorption (max.)	Emission (max.)	pK_a
$(H_3L)^+$	245, 305		3.22(±0.02)
(H_2L)	248, 292		6.0(±0.1)
$(HL)^-$	253. 301		11.6(±0.5)
$(L)^{2-}$	250, 300, 335(sh)		
$[Ru(bpy)_2(H_2L)]^{2+}$	435	630	3.73(±0.03)
$[Ru(bpy)_2(HL^-)]^+$	463	650	11.2(±0.2)
$[Ru(bpy)_2(L^{2-})]^0$	473	670	

comparison with the potentials for the oxidation of similar $Ru(bpy)_2$ complexes containing pyridyl-triazole ligands, the first oxidation step at 0.89 V can be assigned to the oxidation of the metal centre coordinated to the deprotonated triazole ring. For other compounds of the type $[Ru(bpy)_2(LL')]^+$ with LL' = 3-(pyridin-2-yl)-1,2,4-triazole or 3,5-bis(pyridin-2-yl)-1,2,4-triazole, values for this potential of 0.86 and 0.85 V versus SCE were found [17, 18]. By analogy with the free ligand, the peak at 1.26 V is most likely caused by the oxidation of the phenol group and the peak at 1.44 by the further oxidation of the phenoxy radical.

When scanning from 0 to 1.0 V using cyclic voltammetry, a reversible redox wave with $E_{1/2}$ = 0.83 V is observed (Fig. 7(a)). When scanning from 0.0 to 1.8 V, the first oxidation wave was observed at about the same potential, 0.87 V, but now a second oxidation at 1.43 V was present with a peak-to-peak separation of about 310 mV (Fig. 7(b)). On the reverse scan no reduction of the ruthenium centre was observed. This implies that the reduction process of the ruthenium centre is strongly affected by the oxidation of the phenol group.

The above results were further clarified by the use of square wave voltammetry. Using this technique, under suitable scan conditions (e.g. increments of 4 mV and frequency 25 Hz, yielding a scan rate of 100 mV/s), two peaks were detected during the reductive (reverse) scan from 1.8 to 0.2 V. A small peak at *c.* 0.98 V, which is not seen from CV at the same scan rate, is most likely due to reduction of the ruthenium centre. It is noted that during positive scan the oxidation peak area for the ruthenium centre was much bigger than that of the phenol group. However, during the negative scan the peak observed

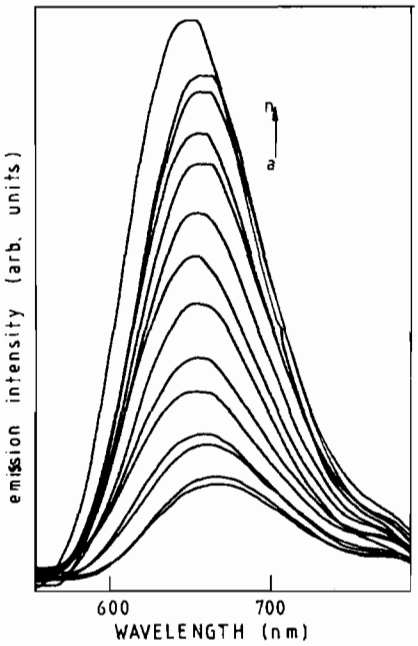

Fig. 5. pH dependence of the emission spectrum of $[Ru(bpy)_2(HL)]PF_6$ (10^{-4} mol dm^{-3}) in an aqueous Britton-Robinson buffer: for curves a to n pH = 12.91, 12.65, 12.16, 11.97, 11.72, 11.52, 11.30, 11.09, 10.84, 10.59, 10.32, 9.93, 9.42, 8.46.

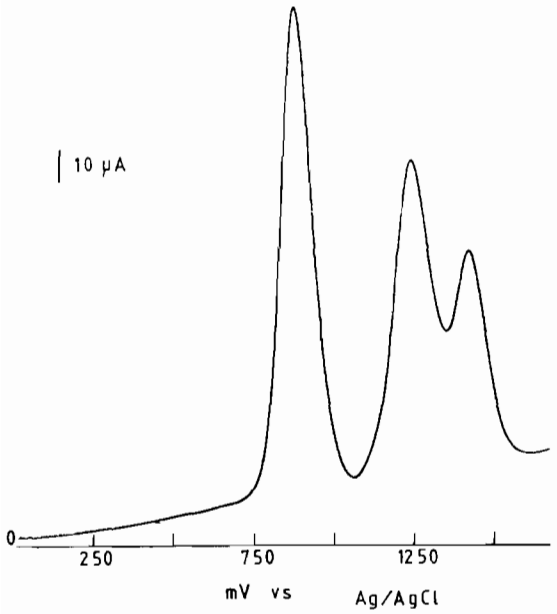

Fig. 6. Differential pulse polarogram of $[Ru(bpy)_2(HL)]PF_6$ in 0.1 M $TEAP/CH_3CN$. Scan rate 5 mV/s, pulse height 50 mV.

for the metal based reduction is very weak, again suggesting that the redox process of the phenol group might physically inhibit the reduction of Ru^{III} to Ru^{II}.

TABLE 5. Electrochemical properties of the $Ru(bpy)_2(H_2L)^{2+}$ compound

E^{DPV} (V)[a]	E^{CV} (V)[b]	E_{pa}	E_{pc}	ΔE_p (mV)	Assignment
1.26[c]	1.27	1.43	1.12	310	phenol oxidation
0.89[c]	0.83	0.86	0.79	70	$Ru^{II} \rightarrow Ru^{III}$
−1.42[c]	−1.52	−1.59	−1.48	110	bpy reduction
−1.68[c]	−1.76	−1.83	−1.72	110	bpy reduction
1.26[d]	irreversible oxidation				phenol oxidation
0.93[d]	0.95	0.99	0.90	90	$Ru^{II} \rightarrow Ru^{III}$
1.15[e]	1.29	1.16	1.42	260	phenol oxidation
0.93[e]	1.03	0.96	1.10	140	$Ru^{II} \rightarrow Ru^{III}$

[a]Measured by DPV, values in volts vs. Ag/AgCl (sat. KCl). [b]Measured by using cyclic voltammetry, values in volts vs. Ag/AgCl (sat. KCl). [c]In 0.1 M $TEAP/CH_3CN$. [d]In 0.1 M aqueous H_2SO_4/CH_3CN. [e]In 0.1 M $TEAP/CH_3CN/CF_3COOH$ (drops).

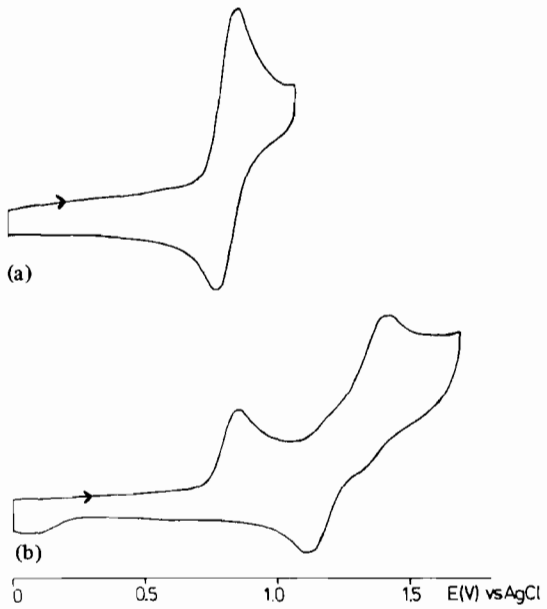

Fig. 7. Cyclic voltammograms of $[Ru(bpy)_2(HL)]PF_6$ in 0.1 M $TEAP/CH_3CN$ with a scan rate 100 mV/s: (a) between 0.0 and 1.1 V vs. Ag/AgCl; (b) between 0.0 and 1.7 V vs. Ag/AgCl.

The effect of the acidity of the electrolyte on the electrochemical behaviour of the ligand and the ruthenium complex was also examined. Upon addition of a few drops of trifluoroacetic acid to the 0.1 M $TEAP/CH_3CN$ electrolyte, the potential for oxidation of the ruthenium centre shifts to about 1.12 V. The peak potentials and peak areas for the phenol group show little change from the non-acidified electrolyte. The shift of the ruthenium redox potential can be explained by the protonation of the triazole ring, as was observed earlier for similar compounds [17, 18]. For the oxidation of the free

ligand, two peaks, which were not clearly separated, were observed at 1.35 and 1.67 V, about 120 mV more positive than in non-acidic electrolytes. The oxidation potential of the free ligand is found at 1.35 V versus Ag/AgCl (sat. KCl), which is somewhat higher than observed in CH_3CN with 0.1 M TEAP.

Both the free ligand and the ruthenium complex were also investigated in the aqueous acidic electrolyte 0.1 M H_2SO_4. The ligand and ruthenium complex were dissolved in a minimum amount of acetonitrile and then added to the acidic solution. Deprotonation of the ligand and complex yielded the same absorption spectra as observed before adding of acid, thus excluding decomposition in the acidic solution. For the ligand, a single broad oxidation peak was observed at *c.* 1.15 V from DPV, which is less positive than that in the aprotic electrolyte (0.1 M TEAP/CH_3CN). For the ruthenium complex three peaks were observed from DPV at 0.93, 1.15 and 1.33 V. The potential for oxidation of the ruthenium centre, 0.93 V, is about 200 mV less positive than that obtained in acified 0.1 M TEAP/CH_3CN, while the phenol based waves are also shifted to less positive values by about 100 mV. More importantly, however, the peak areas of the phenol based oxidations became much smaller. Using cyclic voltammetry, a reversible oxidation wave was observed for the ruthenium centre with a $E_{1/2}$ = 0.95 V (peak-to-peak separation 90 mV) when scanning between 0 and 1.8 V, while no appreciable wave was observed for the phenol oxidation. From UV–Vis spectra obtained in the same medium it was clear that under these conditions the triazole ring is protonated, so that the negative shift of the ruthenium oxidation compared with the potential in acidified CH_3CN can be explained by a solvent shift. From these results it can be concluded that the aqueous acidic electrolyte is unfavourable for the oxidation of the phenol group, with the result that the reduction of Ru^{III} to Ru^{II} is less affected. Apparently, the above two acidic solutions have different effects on the redox behaviour of both the ruthenium centre and the phenol group. The reason for this is not clear at this stage.

Conclusions

The coordination of 3-(2-hydroxy-phenyl)-5-(pyridin-2-yl)-1,2,4-triazole is via N1 of the triazole ring and N of the pyridine ring, while a hydrogen bridge between the phenol ring and N4 is detected. The strong σ-donor capacity of that coordinated site results in a low potential for oxidation of the deprotonated Ru(II) compound. Furthermore, the coordinated ligand is a much stronger acid than the free ligand. Apart from a deprotonation of the triazole ring, a deprotonation of the phenol moiety is also observed for both the free and coordinated ligand.

pH-dependent emission measurements revealed that the excited state pK_a values of $[Ru(bpy)_2(HL)]^+$ are lower than those of the ground state. These observations suggest that excitation takes place from the ruthenium centre to the bpy ligand and not to the pyridyltriazole ligand.

Electrochemical measurements on $[Ru(bpy)_2(HL)]^+$ indicated the presence of an oxidation of the Ru(II) centre and a phenol-based oxidation process. The potential for the oxidation of the Ru(II) centre shifts 200 mV to a higher value upon protonation of the triazole ligand, while the potential for the phenol-based oxidation process hardly changes upon protonation.

Supplementary Material

Atomic coordinates for the hydrogen atoms, thermal parameters, a list of bond distances and angles and a list of calculated and observed structure factors are available from the authors on request.

Acknowledgements

The authors would like to thank Miss Y. Kapteyn for synthesising the ligand. They also wish to thank Johnson Matthey Chemicals Ltd. (Reading, U.K.) for their generous loan of $RuCl_3$. This work was supported in part (A.L. Spek) by the Netherlands Foundation for Chemical Research (SON) and from the Netherlands Organisation for Scientific Research (NWO).

References

1 E. A. Seddon and K. R. Seddon, *The Chemistry of Ruthenium*, Elsevier, Amsterdam, 1984.
2 T. J. Meyer, *Acc. Chem. Res., 11* (1978) 94.
3 T. J. Meyer, *Pure Appl. Chem., 58* (1986) 1193.
4 A. Juris, V. Balzani, F. Barigelletti, S. Campagna, P. Belser and A. von Zelewsky, *Coord. Chem. Rev., 84* (1988) 85.
5 K. Kalyanasanduram, M. Grätzel and E. Pelizetti, *Coord. Chem. Rev., 69* (1986) 57.
6 R. A. Krause, *Struct. Bonding (Berlin), 67* (1987) 1.
7 N. Kitamura, M. Sato, H. B. Kim, R. Obate and S. Tazuke, *Inorg. Chem., 27* (1988) 651.
8 A. Juris, F. Barigelletti, V. Balzani, P. Belser and A. von Zelewsky, *J. Chem. Soc., Faraday Trans. II, 83* (1987) 2295.
9 F. Barigelletti, A. Juris, V. Balzani, P. Belser and A. von Zelewsky, *Inorg. Chem., 26* (1987) 4115.
10 C. D. Tait, R. J. Donohoe, M. K. DeArmond and D. W. Wertz, *Inorg. Chem., 26* (1987) 2754.
11 G. Orellana, M. L. Quiroga and A. M. Braun, *Helv. Chim. Acta, 70* (1987) 2073.
12 D. P. Rillema, D. G. Taghdiri, D. S. Jones, C. D. Keller, L. A. Worl, T. J. Meyer and H. A. Levy, *Inorg. Chem., 26* (1987) 578.
13 J. P. Collin and J. P. Sauvage, *Inorg. Chem., 25* (1986) 135.

14 P. A. Mabrouk and M. S. Wrighton, *Inorg. Chem., 25* (1986) 526.
15 P. J. Steel, F. Lahousse, D. Lerner and C. Marzin, *Inorg. Chem., 22* (1983) 1241.
16 J. G. Vos, J. G. Haasnoot and G. Vos, *Inorg. Chim. Acta, 71* (1983) 155.
17 R. Hage, R. Prins, J. G. Haasnoot, J. Reedijk and J. G. Vos, *J. Chem. Soc., Dalton Trans.,* (1987) 1389.
18 R. Hage, A. H. J. Dijkhuis, J. G. Haasnoot, R. Prins, J. Reedijk, B. E. Buchanan and J. G. Vos, *Inorg. Chem., 27* (1988) 2185.
19 F. H. Case, *J. Org. Chem., 30* (1965) 931.
20 E. J. Browne and J. B. Polka, *J. Chem. Soc. C,* (1968) 824.
21 B. P. Sullivan, D. J. Salmon and T. J. Meyer, *Inorg. Chem., 17* (1978) 3334.
22 G. M. Sheldrick, *SHELXS-86,* a program for crystal structure determination, University of Göttingen, F.R.G., 1986.
23 D. T. Cromer and D. Liberman, *J. Chem. Phys., 53* (1970) 1891.
24 D. T. Cromer and J. B. Mann, *Acta Crystallogr., Sect. A, 24* (1968) 321.
25 G. M. Sheldrick, *SHELX-76,* a program for crystal structure determination, University of Cambridge, U.K., 1976.
26 A. L. Spek, in D. Sayre (ed.), *The Euclid Package. Computational Crystallography,* Clarendon, Oxford, 1982, p. 528.
27 R. Hage, J. P. Turkenburg, R. A. G. de Graaff, J. G. Haasnoot, J. Reedijk and J. G. Vos, *Acta Crystallogr., Sect. C, 45* (1989) 381.
28 D. S. Eggleston, K. A. Goldsby, D. J. Hodgson and T. J. Meyer, *Inorg. Chem., 24* (1985) 4573.
29 D. P. Rillema, D. S. Jones and H. Levy, *J. Chem. Soc., Chem. Commun.,* (1979) 849.
30 R. P. Thummel, F. Lefoulon and J. D. Korp, *Inorg. Chem., 26* (1987) 2370.
31 J. M. Kelly, C. Long, C. M. O'Connell, J. G. Vos and A. H. A. Tinnemans, *Inorg. Chem., 22* (1983) 2818.
32 P. Belser and A. von Zelewsky, *Helv. Chim. Acta, 63* (1980) 1675.
33 J. L. Walsh and B. Durham, *Inorg. Chem., 21* (1982) 329.
34 M. J. Cook, A. P. Lewis, G. S. G. McAuliffe and A. J. Thompson, *Inorg. Chim. Acta, 64* (1982) 125.
35 J. M. Clear, J. M. Kelly, C. M. O'Connell and J. G. Vos, *J. Chem. Res.,* (1981) 3039.
36 F. E. Lytle, L. M. Petrosky and L. R. Carlson, *Anal. Chim. Acta, 57* (1971) 239.
37 A. J. Boulton and A. McKillop, in A. R. Katrinsky and C. W. Rees (eds.), *Comprehensive Heterocyclic Chemistry,* Vol. 5, Pergamon, Oxford, 1984.
38 K. Nakamoto, *J. Phys. Chem., 64* (1960) 1420.
39 F. Barigelletti, L. De Cola, F. Balzani. R. Hage, J. G. Haasnoot, J. Reedijk and J. G. Vos, *Inorg. Chem., 28* (1989) 4344.
40 J. F. Ireland and P. A. H. Wyatt, *Adv. Phys. Org. Chem., 12* (1976) 131.
41 O. Hammerich, in M. M. Baizer and H. Lund (eds.), *Organic Electrochemistry,* Marcel Dekker, New York, 2nd edn., 1983, p. 485, and refs. therein.
42 B. Speiser and A. Ricker, *J. Chem. Res. S,* (1977) 314.
43 J. A. Richards, P. E. Whitson and D. E. Evans, *J. Electroanal. Chem., 63* (1975) 311.
44 B. Speiser and A. Rieker, *J. Electroanal. Chem., 102* (1979) 373.